PHYSICAL REVIEW B VOLUME 61, NUMBER 15 15 APRIL 2000-I

Electronic structures of Na_8Si_{46} and Ba_8Si_{46}

Koji Moriguchi, Mitsuharu Yonemura, and Akira Shintani
Electronics Engineering Laboratories, Sumitomo Metal Industries, Ltd., 1-8 Fusocho, Amagasaki, Hyogo 660-0891, Japan

Shoji Yamanaka
Department of Applied Chemistry, Faculty of Engineering, Hiroshima University, 1-4-1 Kagamiyama, Higashi-Hiroshima, Hiroshima 739-8527, Japan

(Received 13 October 1999)

The effects of Na and Ba atoms doped into silicon clathrate compounds, Na_8Si_{46} and Ba_8Si_{46}, on their energy-band modification have been studied. Both Na and Ba atoms occupy center sites of dodecahedral (Si_{20}) and tetrakaidecahedral cages (Si_{24}), irrespective of the structure of clathrate compounds. Their electronic structures are calculated within the framework of density functional theory. In Na_8Si_{46} clathrate, the Na state is weakly hybridized with the Si_{46} conduction-band state. This weak hybridization results in almost rigid energy-band modification of pristine Si_{46}. In Ba_8Si_{46} clathrate, the conduction band is strongly modified by the Ba state. The Fermi level of Ba_8Si_{46} is located closely to a strong peak of the density of states at the conduction-band edge. Such modification causes the superconductive nature observed in the silicon clathrate doped with Ba.

The existence of two forms of silicon clathrate, Si_{46} and Si_{34} (often referred to as Si_{136}), has been known for three or more decades.[1] Thus far, these compounds have been paid no particular attention except for their crystal structures and chemical properties, because little has been known about their electronic properties and their synthesis was difficult. Since one of the authors has discovered the superconductivity in a metal-doped Si clathrate, $Ba_xNa_ySi_{46}$,[2] the Si clathrates have provoked the interest of many researchers. This interest in Si clathrates may be divided into two viewpoints. One is the similarity to C_{60} compounds and to their related carbon fullerene materials.[3] Since pristine and metal-doped C_{60} have been found to exhibit many interesting properties in terms of geometrical as well as electronic structures,[4] the Si_{46} clathrate, consisting of fullerene units of Si_{20} and Si_{24},[5] is expected to demonstrate similar interesting properties. Actually, superconductivity of metal-doped Si_{46} clathrate has been found, which has been attributed to its cage structure characteristic of C_{60} compounds. The other viewpoint is a wider energy-band gap of pristine silicon clathrates. It is theoretically calculated to have about a 0.7 eV larger gap than a cubic diamond silicon (cd-Si).[5–8] This widening of the band gap is almost the same extent as compared with silicon dots and porous Si, the widening of which is believed to be caused by the quantum effect. Hence, these silicon compounds are potential candidates for optoelectronics, high-power devices, and so on.

The silicon clathrates have been chemically synthesized from Zintl phase compounds such as NaSi and $BaSi_2$.[2,3,9–12] While various synthesis methods have been devised, it is still difficult for the silicon clathrate compounds to be synthesized in a controllable manner to obtain the desired crystal structure and chemical composition. Recently, one of the authors succeeded in the synthesis of barium-doped binary silicon clathrate compounds (Ba_8Si_{46}) utilizing high pressures of up to about 4 GPa.[13] The researchers involved also observed in this silicon clathrate compound a type-II superconductivity with the critical temperature (T_c) of approximately 8 K, which is higher than that of $Na_2Ba_6Si_{46}$ by 4 K.[13] To the authors' best knowledge, this critical temperature is the highest in silicon clathrate compounds reported so far.

The electronic structure of a silicon clathrate compound co-doped with Ba and Na, $Na_2Ba_6Si_{46}$, has been studied using the first-principles calculation by Saito and Oshiyama.[5] Assuming that Ba atoms are to be retained inside the Si_{24} cage and that Na atoms are to be inserted into the Si_{20} unit, they reported that the conduction band is strongly altered and the Fermi-level density of states of $Na_2Ba_6Si_{46}$ becomes higher than expected from a simple filling model of the pristine Si_{46}. They also supposed that this band modification is mainly due to the strong hybridization between the Si_{46} states and the Ba $5d$ states. This high density of states is presumed to be the reason for the superconductivity observed in $Na_2Ba_6Si_{46}$. In contrast to $Na_2Ba_6Si_{46}$, no superconductive nature has been found in Na_8Si_{46}, even at 2 K,[14] in which Na atoms occupy the two inequivalent sites, i.e., the center of the Si_{24} and the Si_{20} cages. There has been no report, however, clarifying the electronic structures of the binary systems such as Na_8Si_{46} and Ba_8Si_{46}. In this report we investigate the electronic structures of these binary systems in order to clarify the difference of the Fermi-level density of states in these clathrate compounds and the resulting superconductive properties. The nondoped pristine Si_{46} crystal is also studied as reference material.

The first-principles calculations for the periodic boundary systems are carried out by means of the *ab initio* pseudopotential theory within the local density approximation (LDA). We use the CASTEP code[15] in order to solve the pseudopotential Schrödinger equation self-consistently. We adopt the ultrasoft pseudopotential proposed by Vanderbilt.[16] The wave functions are expanded on plane-wave basis sets with the kinetic energy cutoff of 300 eV for all the systems studied. The Perdew-Zunger parametrization[17] of the LDA is em-

TABLE I. Crystal structure and inequivalent atomic positions for Si_{46} and Ba_8Si_{46} deduced via geometry optimization. The notation of atomic positions follows that of the International Tables for Crystallography. Experimental values of metal-doped clathrate compounds ($K_{2.9}Ba_{4.9}Si_{46}$) are also listed in the final column. In the present calculation for Na_8Si_{46}, we use the same values as those of Ba_8Si_{46} under the assumption that the Ba atoms are completely substituted by Na atoms.

	Si_{46}	Ba_8Si_{46}	Expt. [a]: $K_{2.9}Ba_{4.9}Si_{46}$
Symmetry	$Pm\overline{3}n(223)$	$Pm\overline{3}n(223)$	$Pm\overline{3}n(223)$
Lattice constant (Å)	10.069	10.192	10.273(1)
Si: $c(6)$	$x=1/4;\ y=0;\ z=1/2$	$x=1/4;\ y=0;\ z=1/2$	$x=1/4;\ y=0;\ z=1/2$
Si: $i(16)$	$x,y,z=0.184$	$x,y,z=0.185$	$x,y,z=0.184(1)$
Si: $k(24)$	$x=0;\ y=0.308$	$x=0;\ y=0.308$	$x=0;\ y=0.305(1)$
	$z=0.117$	$z=0.120$	$z=0.121(2)$
Ba: $a(2)$	–	$x,y,z=0$	$x,y,z=0$
Ba: $d(6)$	–	$x=1/4;\ y=1/2;\ z=0$	$x=1/4;\ y=1/2;\ z=0$

[a] Reference 18.

ployed. As for the Brillouin zone sampling, we adopt 10 special **k** points for the pristine Si_{46} and 20 points for both Na_8Si_{46} and Ba_8Si_{46}. The crystal structures and inequivalent atomic positions used in the present calculations are listed in Table I. The atomistic structures of pristine Si_{46} and Ba_8Si_{46} listed in the table are deduced via geometry optimization. All of the lattice constants calculated here are found to be slightly smaller than those of the experimental values. This fact is not surprising if one uses the LDA approximation. The calculated atomic positions of Ba_8Si_{46}, however, agree well with the experimental values of $K_{2.9}Ba_{4.9}Si_{46}$.[18] In the following calculations for Na_8Si_{46}, we use the same lattice constant as that of Ba_8Si_{46} and assume that the Ba atoms are completely substituted by Na atoms. The two inequivalent center sites, one in the Si_{24} and the other in the Si_{20} cages, are not distinguished, and both sites are filled with Na or Ba in respective clathrate compounds.

The high-resolution transmission electron microscopic (HRTEM) image of the Ba_8Si_{46} prepared by the new high-pressure synthetic method is shown in Fig. 1, together with the schematic diagram of the crystal structure and a multislice simulation image. The multislice simulation depicted in Fig. 1(b) was carried out along the [100] direction of Ba_8Si_{46} with the use of the calculated atomic configurations listed in Table I, assuming a sample thickness of 200 Å and a defocus level of 10 Å. From the viewpoint of the polyhedral space filling in Si_{46} structure, the tetrakaidecahedron (Si_{24}) is a major unit. The HRTEM image clearly exhibits a cage structure of the Si_{24} tetrakaidecahedron, and also shows the arrangement of these cages in the crystal lattice. A computer-simulated atomistic structure inserted in the right hand corner in Fig. 1(c) is in good agreement with the observed image. These results are strong proof that the calculated atomic positions agree well with those of Ba_8Si_{46} prepared by the new high-pressure synthetic method.

The band structure and density of states for Si_{46}, Na_8Si_{46}, and Ba_8Si_{46} are shown in Fig. 2. The total energy difference of pristine Si_{46} from the *cd*-Si is only 0.09 eV/atom, which agrees well with other theoretical predictions.[5–8,19] The band structure of the pristine Si_{46} [Fig. 2(a)] has been well characterized on the basis of theoretical calculations.[5–8,20] We summarize the present results as follows: (i) The fundamental-gap value of Si_{46} is larger than that of *cd*-Si by about 0.7 eV. (ii) The total width of the valence band is narrower than that of *cd*-Si by about 0.9 eV. (iii) A new gap is formed within the valence band. These unique properties of Si_{46} band structure can be attributed to the existence of five-membered rings, since Si 3*s* orbitals cannot form a complete antibonding state, unlike the six-membered rings in *cd*-Si do.

The eight valence electrons from Na atoms in Na_8Si_{46} [Fig. 2(b)] and sixteen electrons from Ba atoms in Ba_8Si_{46} [Fig. 2(c)] contribute to form the conduction-band edge. This

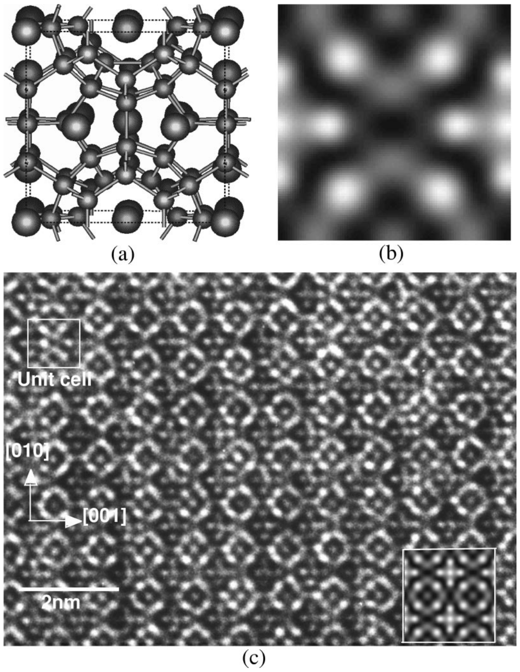

FIG. 1. A TEM image of Ba_8Si_{46} synthesized under a high pressure of 5 GPa. (a) The schematic diagram of the crystal structure of Ba_8Si_{46}. Ba atoms represented by large spheres occupy the center of tetrakaidecahedron and dodecahedron. (b) The multislice simulation image for [100] Ba_8Si_{46} with a specimen thickness of 200 Å and defocus of 10 Å. (c) The HRTEM image obtained with an acceleration voltage of 400 kV. The inset shown in the right corner is the computer-simulated image.

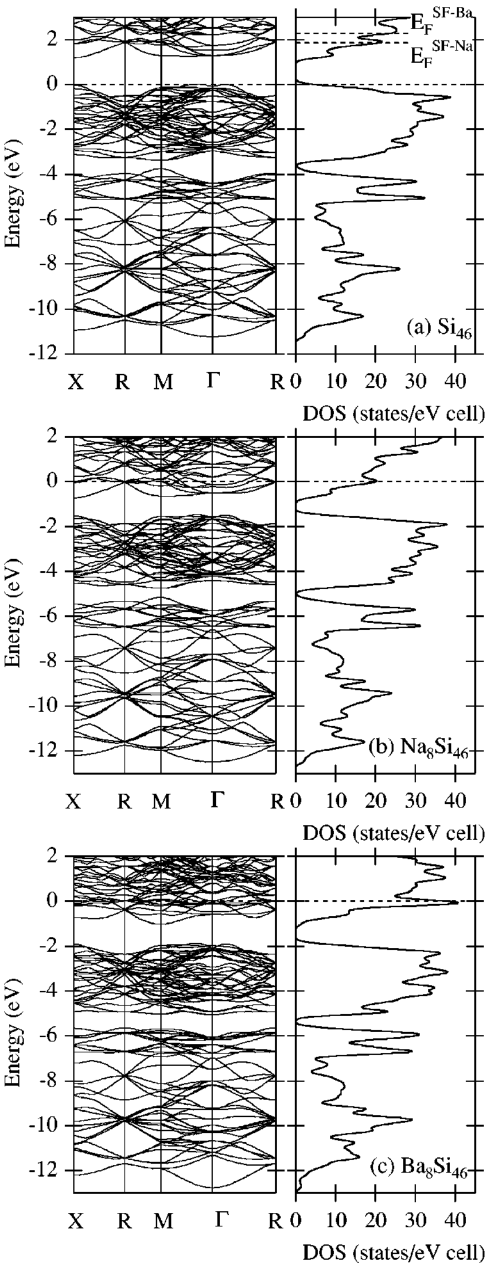

FIG. 2. Band structures and density of states for (a) Si_{46}, (b) Na_8Si_{46}, and (c) Ba_8Si_{46}. Density of states are calculated using 0.1 eV Gaussian broadening of the band structure. Energy is measured from the top of the valence band or the Fermi level, which is denoted by horizontal broken lines. In (a), the energy levels expected from the simple filling of the conduction band of Si_{46} by 8 electrons for Na_8Si_{46} and 16 electrons for Ba_8Si_{46} are denoted by $E_F^{\text{SF-Na}}$ and $E_F^{\text{SF-Ba}}$, respectively.

has a strong effect on the fundamental-energy-gap narrowing in these metal-doped clathrates in comparison with the pristine Si_{46} because of the enhancement of screening effects. Notice that the density of states of Na_8Si_{46} is almost similar to that of the pristine Si_{46}, in not only the valence band but also the conduction band. Moreover, the Fermi-level density of states, $N(E_F)$, of Na_8Si_{46} is almost the same as expected from the simple filling of the conduction band of Si_{46} with eight electrons [Fig. 2(a)]. These findings manifest that Na states are weakly hybridized with the Si_{46} conduction-band states. In contrast, the conduction-band density of states of Ba_8Si_{46} is strongly modified from that of the pristine Si_{46}. The increase in the density of states at the conduction-band edge is remarkable. The Fermi level of Ba_8Si_{46} is located closely to this strong peak as shown in Fig. 2(c). This is caused by the strong hybridization between the Ba states and the Si_{46} conduction band as suggested previously in $Na_2Ba_6Si_{46}$ by Saito and Oshiyama.[5] Compared with the $Na_2Ba_6Si_{46}$, Ba states in binary Ba_8Si_{46} are supposed to contribute more strongly to increase the Fermi-level density of states. Thus, we can assume a higher T_c in Ba_8Si_{46} than in $Na_2Ba_6Si_{46}$. It has been revealed experimentally that the critical temperature of superconductivity in Ba_8Si_{46} is higher than that of $Na_2Ba_6Si_{46}$ by about 4 K.

The difference between Na and Ba atoms in terms of energy state hybridization in the Si_{46} clathrate can be also perceived from different valence-electron density distributions in Na_8Si_{46} and Ba_8Si_{46}. The contour maps of the valence-electron densities of Si_{46}, Na_8Si_{46}, and Ba_8Si_{46} on the (100) plane are shown in Fig. 3. The center site of each figure corresponds to the center of the Si_{20} cage. Both in Na_8Si_{46} and Ba_8Si_{46}, no critical differences have been observed in the electron density distributions, depending on metal-occupying sites (the centers of the Si_{20} or Si_{24} cages). There is, however, a distinct difference in the charge distributions around the metal sites between Na_8Si_{46} [Fig. 3(b)] and Ba_8Si_{46} [Fig. 3(c)]. In Ba_8Si_{46}, the charge distribution around the Ba site is relatively smoothed out and the interaction of Ba with the Si_{46} framework seems to be strong. In contrast, the charge distribution around the Na site is much more localized in Na_8Si_{46}. Therefore, the Ba state is expected to be hybridized more strongly with the Si_{46} conduction-band state than the Na state. From the electronic structure calculations of A_3C_{60} (A=K, Rb, etc.),[21,22] these fullerene compounds exhibit a high $N(E_F)$, which is known to be critical for the occurrence of the superconductivity. The strong hybridization of the Ba state with the Si_{46} conduction-band state and the high $N(E_F)$ play a key role in the superconductivity of barium-doped silicon clathrate compounds. In addition, present results can also explain the absence of the superconductive behavior in Na_8Si_{46}. There has been no report on the experimental determination of charge distributions in silicon clathrate compounds doped with Na or Ba. Based on the present study, these experiments, for which the maximum entropy method (MEM) may be a powerful tool,[23] are interesting.

In summary, we have studied the electronic structures of Na_8Si_{46} and Ba_8Si_{46} within the framework of density-functional theory to elucidate the effect of Na and Ba as a dopant on the energy-band modification in the silicon clathrate compounds. A high-resolution TEM observation of Ba_8Si_{46} has verified the atomic positions that were used for the present calculation. In Na_8Si_{46}, the Na state is found to be weakly hybridized with the Si_{46} conduction-band state, which results in almost rigid energy-band modification of the pristine Si_{46}. In contrast, the conduction band is strongly modified in Ba_8Si_{46}. The Fermi level of Ba_8Si_{46} is found to be close to a peak of the density of states, which should be a critical behavior aspect for the superconductivity observed in

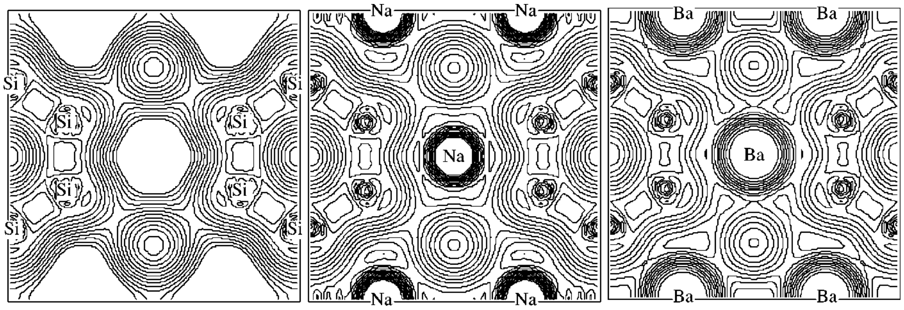

(a)Si_{46} (b)Na_8Si_{46} (c)Ba_8Si_{46}

FIG. 3. Contour maps of the valence-electron densities of (a) Si_{46}, (b) Na_8Si_{46}, and (c) Ba_8Si_{46} on the (100) plane. Each contour represents $1.7^{1/2}$ $(1/1.7^{1/2})$ times the density of the neighboring contours. The maximum contour of the density is set to 1 electron/Å^3. In (a), the core regions of silicon atoms forming half hexagons are indicated on both sides of the figure by the letters ''Si.'' The center of the figure corresponds to the center hole of the Si_{20} cage. The Si-Si bonds perpendicular to the (100) plane correspond to spherical regions with relatively high electron density above and below the center. In (b) and (c), sodium and barium atom sites are denoted by the letters ''Na'' and ''Ba,'' respectively.

Ba-doped silicon clathrates. It is expected that the electronic density of states around the Fermi level increases with the Ba concentration in Ba-doped silicon clathrate compounds. Considering the absence of the superconductve behavior in Na_8Si_{46}, we also suggest that the estimation of Fermi density of states from the band-structure calculation and the analysis based on the BCS theory are quite effective for predicting the superconductivity in silicon clathrate compounds.

The HRTEM observation of Ba_8Si_{46} was performed by K. Hanafusa (Sumitomo Metal Industries, Ltd.). We would like to thank S. Munetoh, S. Shibagaki, and Dr. K. Kamei for helpful discussions. Special thanks are due from one of the authors, K. M., to Dr. N. Sano and L. M. Parish for a critical reading of the manuscript. The author's gratitude also goes to Dr. S. Kobayashi for his encouragement with this research.

[1] J. Kasper, P. Hagenmuller, M. Pouchard, and C. Cros, Science **150**, 1713 (1965).

[2] H. Kawaji, H. Horie, S. Yamanaka, and M. Ishikawa, Phys. Rev. Lett. **74**, 1427 (1995).

[3] K. Tanigaki, O. Zhou, and S. Kuroshima, in *Proceeding of the International Winterschool on Electronic Properties of Novel Materials. Fullerenes and Fullerene Nanostructures* (World Scientific, Singapore, 1996), p. 475.

[4] *The Fullerenes*, edited by H. W. Kroto, J. E. Fischer, and D. E. Cox (Pergamon Press, Oxford, 1993).

[5] S. Saito and A. Oshiyama, Phys. Rev. B **51**, 2628 (1995).

[6] G. B. Adams, M. O'Keeffe, A. A. Demkov, O. F. Sankey, and Y. M. Huang, Phys. Rev. B **49**, 8048 (1994).

[7] A. A. Demkov, O. F. Sankey, K. E. Schmidt, G. B. Adams, and M. O'Keefe, Phys. Rev. B **50**, 17 001 (1994).

[8] M. Menon, E. Richter, and K. R. Subbaswamy, Phys. Rev. B **56**, 12 290 (1997).

[9] P. P. Mélinon, P. Kéghélian, X. Blase, J. Le Brusc, A. Perez, E. Reny, C. Cros, and M. Pouchard, Phys. Rev. B **58**, 12 590 (1998).

[10] F. Shimuzi, Y. Maniwa, K. Kume, H. Kawai, S. Yamanaka, and M. Ishikawa, Phys. Rev. B **54**, 13 242 (1996).

[11] S. Yamanaka, H. Horie, H. Nakano, and M. Ishikawa, Fullerene Sci. Technol. **3**, 21 (1995).

[12] S. Yamanaka, H. Kawaji, and M. Ishikawa, Mater. Sci. Forum **232**, 103 (1996).

[13] S. Yamanaka, E. Enishi, H. Fukuoka, and M. Yasukawa, Inorg. Chem. **39**, 56 (2000).

[14] S. B. Roy, K. E. Sim, and A. D. Caplin, Philos. Mag. B **65**, 1445 (1992).

[15] The CASTEP code is available from Molecular Simulations Inc.

[16] D. Vanderbilt, Phys. Rev. B **41**, 7892 (1990).

[17] J. P. Perdew and A. Zunger, Phys. Rev. B **23**, 5048 (1981).

[18] S. Yamanaka, H.-O. Horie, H. Kawaji, and M. Ishikawa, Eur. J. Solid State Inorg. Chem. **32**, 799 (1995).

[19] M. O'Keeffe, G. B. Adams, and O. F. Sankey, Philos. Mag. Lett. **78**, 21 (1998).

[20] A. A. Demkov, W. Windl, and O. F. Sankey, Phys. Rev. B **53**, 11 288 (1996).

[21] S. Saito and A. Oshiyama, Phys. Rev. B **44**, 11 536 (1991).

[22] S. Saito and A. Oshiyama, J. Phys. Chem. Solids **54**, 1759 (1993).

[23] M. Fujimori, T. Nakata, T. Nakayama, E. Nishibori, K. Kimura, M. Takata, and M. Sakata, Phys. Rev. Lett. **82**, 4452 (1999).